Bull. Nov. Comp. Center, Num. Model. in Atmosph., etc., 9 (2004), 17–27

Modeling of land hydrology with the use of topographical features*

V.N. Krupchatnikoff, A.I. Krylova

Introduction

For the last few years, much progress has been made towards representing the hydrology processes in the land-surface parameterization schemes [1–4]. With an increased interest in the prediction of runoff and soil moisture under the current and changed climate conditions, an understanding has been that the parameterization of the runoff-related processes needs to explicitly account for the topographical control. The land surface model (LSM) for the atmospheric general circulation model (GCM), after integrating with a topography-based runoff scheme is able to produce the topography-related runoff and river discharge [5].

The primary purpose of this study is to correct the parameterization scheme surface hydrology and to include a model of the river routing of the terrestrial runoff into the oceans. The total runoff (surface and subsurface drainage) is routed downstream to the oceans using a river routing model. The river routing model is based on the TOPMODEL ideas [6]. The river routing model is coupled to the Land Surface Model (ICM&MG SB RAS) for hydrological applications and for the improved land-ocean-sea-ice-atmosphere coupling in the Climate System Model (CSM).

1. The topography-based hydrological model (TOPMODEL)

1.1. The basic TOPMODEL approach. Numerous field studies have indicated that the surface runoff in wet regions is mainly produced by the saturation excess runoff (the Dunne flow). This means that the spatial distribution of the soil moisture storage will result in different surface runoff production. The saturation excess runoff will occur in a certain part of a large area where there is no soil moisture deficit or the groundwater goes up to the ground surface. The data have shown that within a catchment a substantial soil moisture heterogeneity exists at almost any scale and that major control of the soil moisture distribution is topography [6]. There are many surface runoff models based on the saturation excess runoff mechanism, but only a few models take into consideration the topography influence on the spatial distribution pattern of the soil moisture, and, in turn, on the runoff

*Supported by the Russian Foundation for Basic Research under Grant 03-05-96828.

production. The TOPMODEL fully takes into the consideration the influence of topography on the soil moisture and the groundwater table over a catchment. Using the *a priori* computed topographical index of a catchment and average water storage deficit calculated in the drainage, TOPMODEL directly estimates spatial distributions of the groundwater table and a local water storage deficit in the unsaturated zone, and predicts the portion of an area in the catchment, where the saturation excess runoff will occur.

1.2. The basic equations of TOPMODEL. The TOPMODEL simulates a runoff based on the variable source area concept of streamflow generation. Three mechanisms constitute the variable source area concept: saturation overland flow from direct precipitation on saturated land surface areas, saturation overland flow from the return flow of subsurface water to the surface in the saturated areas, and the subsurface interflow.

In TOPMODEL, the total streamflow is the sum of the saturation overland flow and the subsurface flow

$$Q_{\text{total}} = Q_{\text{overland}} + Q_{\text{subsurface}}. \tag{1}$$

The saturation overland flow is the sum of direct precipitation on saturated areas and the return flow

$$Q_{\text{overland}} = Q_{\text{direct}} + Q_{\text{return}}. \tag{2}$$

Expressions for computing specific flows are derived from the continuity equation and Darcy's law.

In TOPMODEL [6], there are three basic assumptions:

1. Steady-state conditions (inflow = outflow) and a spatially uniform recharge rate R to the water table:

$$a_i \cdot R = T \cdot \tan\beta, \tag{3}$$

   where $a_i = A_i/c$, A_i is a draining area through the location i, c is the contour width (a length perpendicular to the flow direction), T is the soil transmissivity, and $\tan\beta$ is the slope of the land surface;

2. The slope of the water table is assumed to be as that of the land surface so that the local hydraulic gradient be close to $\tan\beta$;

3. The saturated hydraulic conductivity K_z exponentially decreases with depth: $K_z = K_0\, e^{-fz}$, where K_0 is the hydraulic conductivity at the soil surface and f is a parameter that governs the rate of a decrease of K with depth.

According to the above three assumptions, $q_{\text{subsurface},i}$ beneath the water table at any point i in a catchment is determined by

$$q_{\text{subsurface},i} = T_0\, e^{-s/m} \tan\beta, \tag{4}$$

where s is the saturation deficit, $T_0 = K_0/f$, $m = n/f$, n is the porosity fraction of the soil. From (3) and (4), we have

$$q_{\text{subsurface},i} = a_i\, R = T_0\, e^{-s/m} \tan\beta. \tag{5}$$

Having solved s in (5), we obtain

$$s = -m \ln \frac{R}{T_0} - m \ln \frac{a_i}{\tan\beta}. \tag{6}$$

To solve the average saturation deficit for a catchment, equation (6) is integrated over the catchment and divided by the area

$$\overline{s} = \frac{1}{A} \int_0^A s\, di$$

or, assuming that R and T_0 are constant over the catchment:

$$\overline{s} = -m \ln \frac{R}{T_0} - m \frac{1}{A} \int_0^A \ln \frac{a_i}{\tan\beta}\, di. \tag{7}$$

Defining λ as mean $\ln(a/\tan\beta)$ (a topographical index) for the catchment and combining equation (7) with equation (6), we arrive at

$$s = \overline{s} + m \left[\lambda - \ln \frac{a_i}{\tan\beta}\right]. \tag{8}$$

Equation (8) is the TOPMODEL equation. It permits the reconstruction of a spatial variability of the catchment response to meteorological forcing solely from the modeling of the response of the mean state.

Equation (8) is used to determine the overland flow (2). The direct runoff flow is generated when precipitation falls on a saturated area:

$$q_{\text{direct}} = \frac{A_{\text{sat}}}{A}\, P.$$

Here A_{sat}/A is calculated by computing s at any point. If s is less than or equal to zero, the soil is completely saturated and any rain on the surface will become a direct overland flow. This most easily occurs for the points within the catchment, where the topographical index is large. The return flow occurs where s is less than zero. The rate of the return flow is given by:

$$q_{\text{return}} = |s|\, \frac{A_{\text{sat}}}{A}.$$

To compute the mean subsurface discharge, $q_{\text{subsurface}}$ is integrated along the length of all stream channels and divided by the catchment area:

$$\overline{q}_{\text{subsurface}} = \frac{1}{A}\int_L T_0\, e^{-s/m} \tan\beta\, dL$$

or

$$\overline{q}_{\text{subsurface}} = T_0\, e^{-\lambda}\, e^{-\overline{s}/m}.$$

Other components of the TOPMODEL like evapotranspiration, interception, etc., are not *a priori* defined.

The temporal resolution of the TOPMODEL is not fixed. The processes in the model can be simulated at any time step. However, the temporal resolution of data needs to match the time scale of the dynamics in the theoretical framework of the model, and this time scale is thought to be in the order of hours.

1.3. Discussion of the topographical index. The topographical index, $\ln(a/\tan\beta)$, quantitatively captures the effect of topography on the development of saturation areas in a catchment. A map of topographical indices for a catchment, calculated from the DEM (digital elevation model) of a catchment, shows the areas where the runoff processes such as saturation-excess overland flow are likely to occur. High values of the topographical index indicate to the areas with large contributing zones and relatively flat slopes, typically at the base of hillslopes and near the stream. Low topographical index values are found at the tops of hills, where there is a relatively small upslope contributing area.

There are two factors which affect a pattern of the topographical index distribution: the resolution of the topography used in the DEM and the way to define a grid as containing a river channel or not in a catchment. In this paper, the effect of the first factor is considered.

Figure 1 shows the calculated curve of the topographical index distribution density, based on the GTOPO30 DEM with 1000 m $\times$ 1000 m resolution data of topography elevation in the Tom river basin. From the figure, it can be seen that a maximum topographical index is larger in mountainous regions than in flat areas. The distribution function $\ln(a/\tan\beta)$ is influenced by the spatial resolution as follows: distributions in flat areas are smoother than those in mountainous regions.

In work [7], a regression equation was proposed to relate values of the topographical index at 1000 m resolution to that at 100 m resolution as follows:

$$\lambda_{100\,\text{m}} = 0.961\,\lambda_{1000\,\text{m}} - 1.957.$$

We consider the topographical index values at 10- minute resolution and at 30-second resolution. It turns out that this idea may work for these scales:

$$\lambda_{10'} = -0.07 + 1.62\,\lambda_{30''}. \tag{9}$$

Figure 2 shows the regression relationship (9).

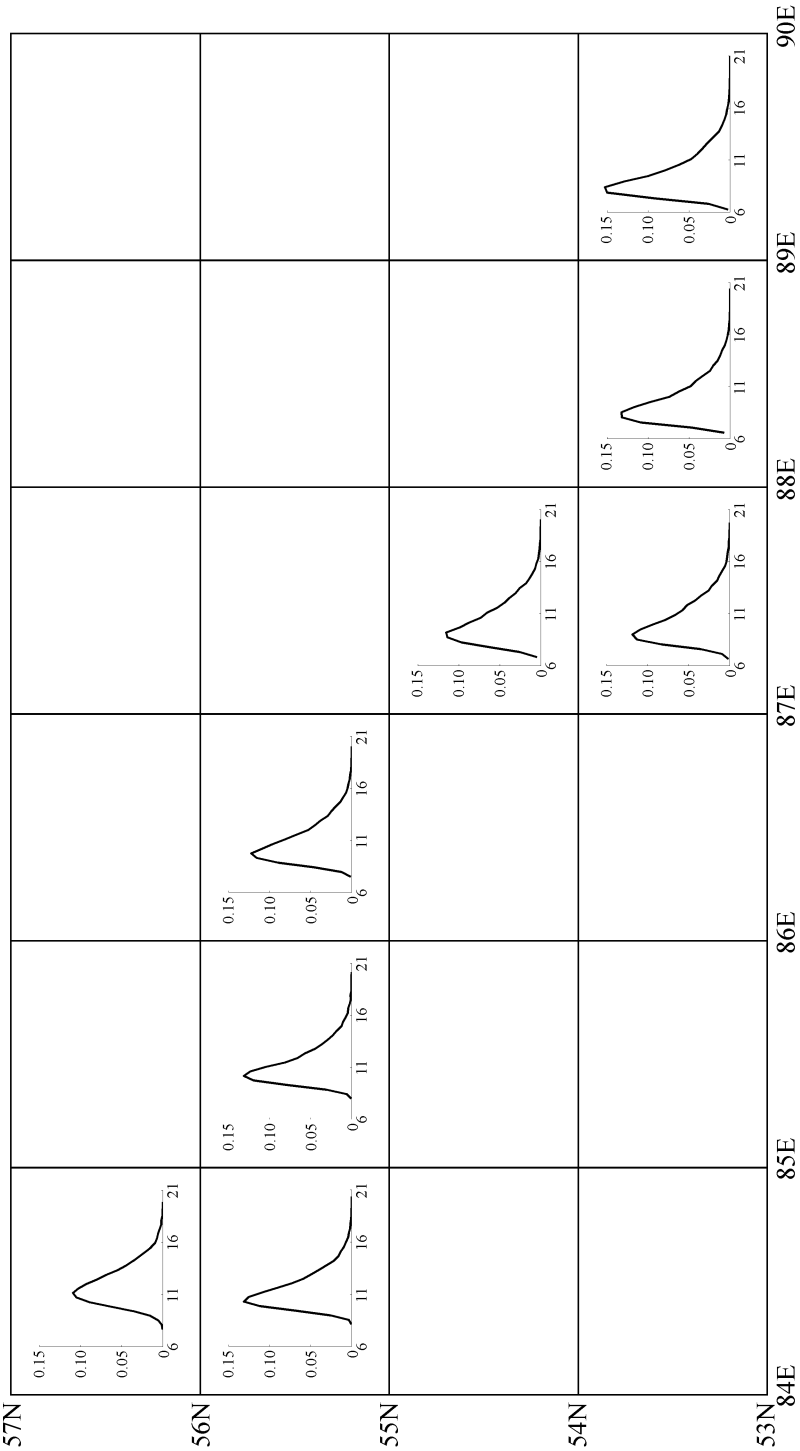

Figure 1. The topographic index computed from GTOPO30 DEMs for the Tom river basin

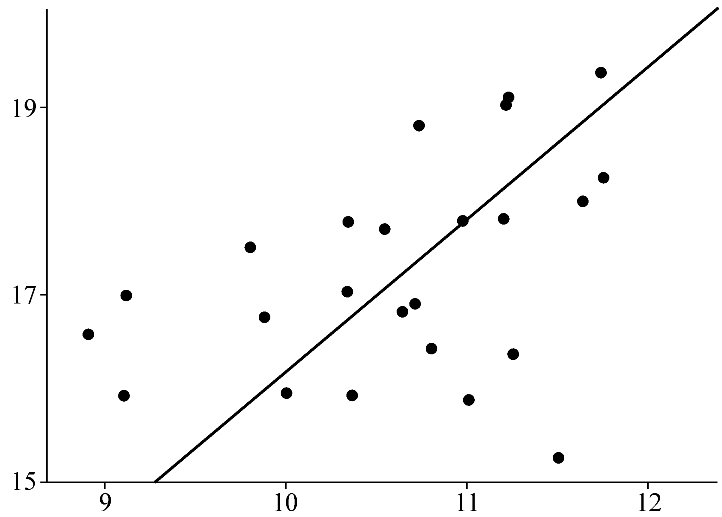

Figure 2. Upscaling function for obtaining $10'$ equivalent of a topographical index from its values for 30-arc-second DEM

2. The topography-related runoff model

In order to focus on the topographical effects the topography-related runoff model in this paper does not include a canopy water component, snow, surface runoff and infiltration described in [8].

2.1. Saturated hydraulic conductivity. The parameterization follows closely the TOPMODEL framework [6] and the work by Stieglitz et al. [5]. The saturated hydraulic conductivity decreases with depth according to

$$K_{\text{sat}}(z) = K_{\text{sat}}(0)\, e^{-fz},$$

where z is a soil depth, $K_{\text{sat}}(0)$ is the surface value of the saturated hydraulic conductivity, and $1/f$ is e-folding depth of K_{sat} can be determined through the optimization procedure. In the ICM&MG land-surface model, the soil moisture is calculated at the interface level of the model layers

$$q_{i+1/2} = -k_{i+1/2}\left(\frac{\psi_{i+1} - \psi_i}{\Delta z_{i+1/2}} - 1\right), \qquad k_{i+1/2} = \frac{2\Delta z_{i+1/2}}{\Delta z_i/k_i + \Delta z_{i+1}/k_{i+1}},$$

$q_{i+1/2}$ is a soil moisture flux at the interface level between the layers i and $i+1$, ψ_i, Δz_i are matrix potential and the layer thickness of the layers i and $i+1$. Hydraulic conductivity k and soil matrix potential ψ depend on the volumetric soil water content θ ($\mathrm{m}^3/\mathrm{m}^3$) and a soil texture. For the i-th layer [9]

$$k_i = k_{\text{sat}} \frac{\theta_i}{\theta_{\text{sat}}}, \qquad \psi_i = \psi_{\text{sat}} \left(\frac{\theta_i}{\theta_{\text{sat}}} \right)^{-b},$$

where k_{sat} is hydraulic conductivity at saturation k (mm/s), ψ_{sat} is a matrix potential at saturation (mm), water content at the saturation θ_{sat} (porosity), and b are empirically related to percentage of sand and clay. Hydraulic conductivity at the saturation k_{sat} varies with percentage of sand according to [10] $k_{\text{sat}}(0) = 0.0070556 \cdot 10^{-\alpha+\beta}$, where α and β can be determined through optimization procedures.

2.2. Bottom drainage. The gravitational loss of soil water from the bottom of the model soil column is given by the following: for the bottom layer $i = 6$,

$$q_6 = -k_6^n - \frac{dk_6}{d\theta_6} \Delta\theta_6.$$

2.3. Saturation excess. The soil water may exceed the physical constraints. Any soil in excess of saturation

$$\sum_i (\theta_i - \theta_{\text{sat}}) \Delta z_i = W_{\text{ex}}$$

is added to the soil, starting at the top of the soil layer. Any remaining excess water is added to the subsurface drainage $q_{i,\text{drain}}$ (the subsurface runoff). This saturation excess is used to recharge the soil layers above a water table.

If a column becomes oversaturated, the subsurface runoff due to a saturation excess is

$$R_{\text{sat,sb}} = \max \left\{ 0, \ \sum_i (\theta_i - \theta_{\text{sat}}) \frac{\Delta z_i}{\Delta t} \right\}.$$

The water table depth z_{wt} is used to determine a saturated function, a surface runoff and a baseflow. The method proposed in [10] can be used here to evaluate a water table. Assuming that there is no vertical moisture flux, then total head must be conserved within the soil column $\psi(z) - z = \psi_{\text{sat}} - z_{\text{wt}}$, or

$$\psi_{\text{sat}} \left(\frac{\theta(z)}{\theta_{\text{sat}}} \right)^{-b} - z = \psi_{\text{sat}} - z_{\text{wt}}.$$

The water table depth z_{wt} is then computed by the iterative solution of the equality

$$W_{\text{ex}} = \int_0^{z_{\text{wt}}} (\theta_{\text{sat}} - \theta(z)) \, dz.$$

2.4. Subsurface runoff. For focusing on the topographical effect of the new version of the land-surface model, we describe only a modified surface and subsurface runoff components of the land hydrology model. The surface runoff consists of an overland flow by the Dunne and the Horton mechanism, the topographical effect on runoff processes having a mathematical representation. The mathematical representation of the surface runoff takes in the form of

$$R = \eta_s R_{s>1} + (1-\eta_s) R_{s<1},$$

where

$$\eta_s = \int_{|\overline{\lambda}+f z_{\rm wt}|<\lambda} \varphi(\lambda)\, d\lambda, \qquad s = \frac{\theta}{\theta_{\rm sat}},$$

$\overline{\lambda}$ is a mean value of λ in a grid cell, $\varphi(\lambda)$ is a probability density function of λ, $z_{\rm wt}$ is a mean grid cell of the water table depth. The subsurface runoff is parameterized in the form

$$R_{\rm sub} = R_{{\rm sub},\lambda} + R_{\rm sub,drain} + R_{\rm sub,ex},$$

where $R_{{\rm sub},\lambda}$ is a subsurface runoff due to the topographical control (calculated by the TOPMODEL), $R_{\rm sub,drain}$ is a bottom drainage, and $R_{\rm sub,ex}$ is a saturation excess.

2.5. Topographical control. The subsurface runoff due to the topographical control is given by

$$R_{{\rm sub},\lambda} = \alpha \frac{K_{\rm sat}(0)}{f}\, e^{-(\overline{\lambda}+f z_{\rm wt})},$$

where λ is a factor with allowance for a difference in the saturated hydraulic conductivity in the lateral and in the vertical directions [10].

3. The river discharge model

Discharges from most of the world's largest rivers have large annual cycles. For example, the Amazon peaks in May-June, the Orinoco peaks in August, the Changjiang peaks around July; whereas large Siberian rivers (Yenisey, Lena, Ob) have a sharp peak in June arising from snowmelt. The basin wide integrated precipitation does not usually have the same seasonal phase as for the river discharge, which illustrates important effects of the snow accumulation and melting and the river transport. The total discharge into the Arctic peaks in June, whereas the peak is in May for the Atlantic Ocean and in August for the Indian Ocean. Snow accumulation and melt have essential effects on the annual cycle of discharge into the Arctic, the Atlantic, the Pacific, and the global oceans, but little influence on the discharge into the Indian Ocean and the Mediterranean and the Black Seas. The long-term mean values of the river runoff and the continental discharge reported here is available for the free download from NCAR's Climate Analysis Section catalog (http://www.cgd.ucar.edu/cas/catalog/).

In order to estimate the continental discharge into any ocean basin, we should sum up the river outflow within each ocean basin. We have decided to use some ideas of the river routes water models to estimate the river outflow [11, 12]. Using a linear advection scheme with 100 resolution river rout water model from one cell to its downstream neighboring cell by considering the balance of horizontal water inflows and outflows:

$$\frac{\Delta W_{\text{riv}}}{\Delta t} = \sum_i F_{\text{in},i} - F_{\text{out}} + R,$$

where $F_{\text{out}} = \overline{\frac{\partial \upsilon_r}{\partial l}}\, W_{\text{riv}}$ is a divergence source of the river water, $\overline{\frac{\partial \upsilon_r}{\partial l}} \approx \frac{\upsilon_r^*}{d}$, υ_r^* is the effective water flow velocity [13]; W_{riv} is the stream water storage within the cell (m^3); F_{out} is a water flux leaving the cell in the downstream direction (m^3/s); $\sum_i F_{\text{in},i}$ is the sum of inflows of water from upstream cells (m^3/s); R is runoff, r is a distance between the centers of a cell and its downstream neighboring cell (m). It takes some time to reach equilibrium under constant runoff field. Estimation of this time is about 5–6 years with $\upsilon_m = 0.5$ m/s starting with an empty river channel.

Therefore, we should use a river flow after 1800 model days in annual simulations. The total runoff (surface and sub-surface drainage) is routed downstream to the oceans using a river routing model. River routing model is based on TOPMODEL ideas [6]. A river routing model is coupled to the Land Surface Model (ICM&MG SB RAS) [4] for hydrological applications and for an improved land–ocean–sea ice–atmosphere coupling in the Climate System Model (CSM). We have implemented this model on a 1-degree grid. The land model interpolates the total runoff from the column hydrology (2.8 by 2.8 degree) to the river routing 1-degree grid. Figure 3 shows here the result of a regional 1° by 1° off-line simulation (the River Tom basin) using global ICM&MG LSM. The model is driven with AMIP data from 1979 to 1993.

Conclusion

We have prepared a new version of the surface hydrology parameterization scheme that will be able to estimate the continental freshwater discharge into the oceans. The first thing we are planing to do is to prepare the discharge data from the ocean-reaching rivers selected from several comprehensive streamflow data sets. The drainage area of these rivers is $79.53 \cdot 10^6$ km^2, or about 68% of the global non-ice, nondesert land areas. Also, we are going to estimate the river mouth outflow from the Siberian large rivers (Ob,

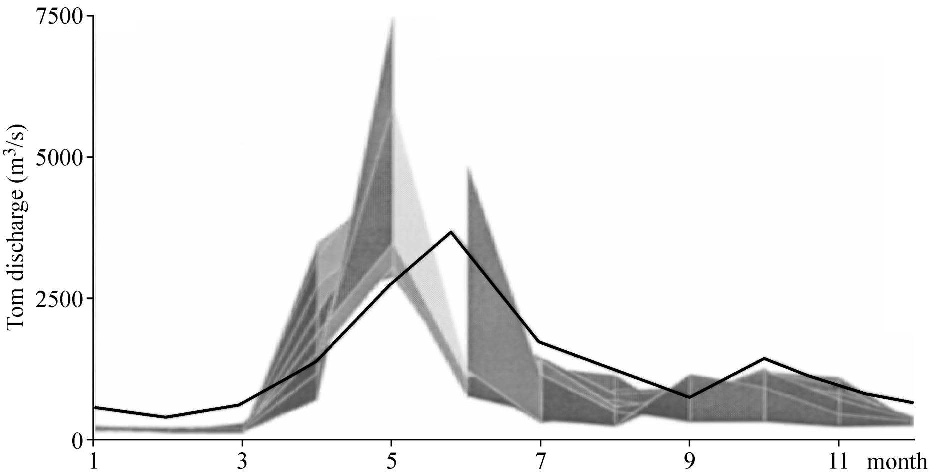

Figure 3. Seasonal water discharge of the Tom river. The solid line – the model result (off-line simulation). Clauster of lines – observations of discharge for period of 1965–1984 years

Yenisei, Lena) by adjusting the streamflow rate at the farthest downstream stations using the ratio of simulated flow rates at the river mouth and the station. The discharge from the unmonitored areas was estimated based on the ratios of the runoff and drainage area between the unmonitored and the monitored areas at any latitude. Second, we are also going to compute the annual continental discharge into the Arctic Ocean by forcing the river waterflux model with the P–E fields derived from the NCEP and the ECMWF reanalysis with a adjustment for snow effects.

References

[1] Bonan G.B. A land surface model (LSM version 1.0) for ecological, hydrological and atmospheric studies: technical description and user's guide. — NCAR Tech. Note NCAR/TN-417+STR, 1996. (Available from NCAR, P.O.Box 3000, Boulder, CO 80307.)

[2] Bonan G.B. The land surface climatology of the NCAR land surface model coupled to the NCAR-Community Climate Model // J. Climate. — 1998. — Vol. 11. — P. 1307–1326.

[3] Alekseev V., Volodin E., Galin V., Dymnikov V., Lykossov V. Modeling current climate using atmospheric general circulation model of INM RAS: Model description. — Moscow, 1998. — (Preprint / INM RAS).

[4] Krupchatnikoff V. Simulation of CO2 exchange processes in the atmosphere surface biomes system by climate model ECSib // Russ. J. Numer. Anal. Math. Modelling. — 1998. — Vol. 13, No. 6. — P. 479–492.

[5] Stieglitz M., Rind D., Famiglietti J.S., Rosenzweig C. An efficient approach to modeling the topographic control of surface hydrology for regional and global climate modeling // J. Climate. — 1997. — Vol. 10. — P. 118–137.

[6] Beven K.J., Kirkby M.J. A physically-based variable contributing area model of basin hydrology // Hydrol. Sci. Bull. — 1979. — Vol. 24. — P. 43–69.

[7] Wolock D.M., McCabe G.J.Jr. Differences in topographic characteristics computed from 100- and 1000-meter resolution digital elevation model // Hydrol. Process. — 2000. — Vol. 14. — P. 987–1002.

[8] Krupchatnikoff V.N., Krylova A.I. Numerical modeling of surface hydrology in coupled climate model // Proc. Intern. Conf. on Computational Mathematics ICCM-2004. Part II. — Novosibirsk, 2004. — P. 882–889.

[9] Clapp R.B., Hornberger G.M. Empirical equations for some soil hydraulic properties // Water Resour. Res. — 1978. — Vol. 14. — P. 601–604.

[10] Chen J., Kumar P. Topographic influence on the seasonal and interannual variation of water and energy balance of basins in North America // J. Climate. — 2001. — Vol. 14. — P. 1989–2014.

[11] Hagemann S., Dumenil L. A parameterization of the lateral waterflow for the global scale // Clim. Dyn. — 1998. — Vol. 14. — P. 17–31.

[12] Kuzin V.I. Hydrological aspects in modeling of Siberian climate // Proc. Intern. Conf. of Mathematical Methods in Geophysics MMG-2003. Part II. — Novosibirsk, 2003. — P. 323–327.

[13] Miller J.R., Russell G.L., Caliri G. Continental-scale river flow in climate models // J. Climate. — 1994. — Vol. 7. — P. 914–928.